Computers in Biology and Medicine 114 (2019) 103433

Contents lists available at ScienceDirect

Computers in Biology and Medicine

journal homepage: http://www.elsevier.com/locate/compbiomed

Encapsulation efficiency of single-walled carbon nanotube for Ifosfamide anti-cancer drug

Mehdi Yoosefian [a,*], Sakineh Sabaei [a], Nazanin Etminan [b]

[a] Department of Nanotechnology, Graduate University of Advanced Technology, Kerman, Iran
[b] Chemistry Department, University of Payam-noor, 19395-4697, Tehran, Iran

ARTICLE INFO

Keywords:
Ifosfamide
Drug delivery
Encapsulation
Single-walled carbon nanotubes
Conformer
Solvent effect

ABSTRACT

The encapsulation efficiency of (10,10) armchair single-walled carbon nanotubes as a nanovector for Ifosfamide anti-cancer drug has been investigated. (10,10) armchair single-walled carbon nanotube was selected because of larger inner volume for encapsulation, distinct inner and outer surfaces for functionalization and penetration possibility into cells or cell nucleus. Moreover, the adverse side effects of Ifosfamide can be reduced by single-walled carbon nanotubes. A complete understanding of the encapsulation process of drug molecules into carbon nanotubes is necessary for drug delivery development. All possible stable conformers of the drug have been investigated through geometry optimizations at the B3LYP/6-31G**level of theory by using the Gaussian 09 suite of programs and then encapsulation of the most stable conformer has been studied. Results show that the Ifosfamide drug molecule can be encapsulated into the internal cavity of armchair single-walled carbon nanotube. The corresponding adsorption energy is −3.87 eV. Furthermore, the effects of encapsulation on the electronic properties of the carbon nanotube such as equilibrium distances, HOMO–LUMO energy gap and DFT based descriptors have been also probed. Quantum mechanical calculations of encapsulation verify that a single-walled carbon nanotube could adsorb an Ifosfamide molecule spontaneously via the chemisorption process.

1. Introduction

Ifosfamide (IFO), 3-(2-Chloroethyl)-2-[(2-chloroethyl) amino] tetrahydro-2H-1,3,2- oxazaphosphorine -2-oxide, that was first developed at Asta-Werke in Germany, is one of the oxazaphosphorine class of alkylating agents that exhibits antitumor and immunomodulatory activities. Ifosfamide clinical activity in various cancers has been verified. Its dose-limiting toxicity is due to biotransformation that leads to highly reactive metabolites such as acrolein and chloroacetaldehyde. Healthy rapid dividing cells could be targeted to chemotherapy drugs to cause systemic toxicity for patients. But a high administered dosage has been resulted in high neurotoxicity, nephrotoxicity, urotoxicity, encephalopathy and cardiotoxicity [1].

Nanomaterials have been increasingly investigated in the biomedical field [2–5]. Recent researches in nano encapsulation have provided drug delivery systems that increase the efficacy, specificity and targeting ability of therapeutic agents [6–8]. Nanocapsules with efficient drug molecule loading could reduce systemic toxicity and enhance the accumulation of drug at the target site. On the one hand, adverse side effects will be reduced and healthy normal cells will be protected from chemotherapy treatment. On the other hand, the drug could be protected from environmental impacts [9–11] by nano encapsulation until they reach the target site that results in long-term stability [12].

Carbon nanotubes (CNT), which are novel inflexible non-polar candidates for encapsulation, first discovered by Ijima in 1991 [13]. They show promising environmental [10], biological [14] and medical [15] applications. They offer excellent characteristics due to mechanical strength, high chemical stability and electrical properties [16–19]. They could often be taken up by cells without the immune system recognition due to their small size and high aspect ratio. Carbon nanotubes with large accessible inner volume and open ends could be a promising alternative nanocarrier [20–23]. Spontaneous encapsulation of biomolecules and drugs into the inner space of CNTs have been reported [12]. Functionalization, toxicity of CNTs and pharmacology are the most important limitation of carbon nanotubes in biological and biomedical environments which should be overcome. Surface modification with different hydrophilic molecules and other agents may increase the biocompatibility and water solubility of CNTs. Physical and chemical properties of armchair carbon nanotubes such as size, shape, aggregation, chemical composition, functionalization and solubility could be

* Corresponding author.
E-mail address: m.yoosefian@kgut.ac.ir (M. Yoosefian).

https://doi.org/10.1016/j.compbiomed.2019.103433
Received 3 May 2019; Received in revised form 2 September 2019; Accepted 3 September 2019
Available online 4 September 2019

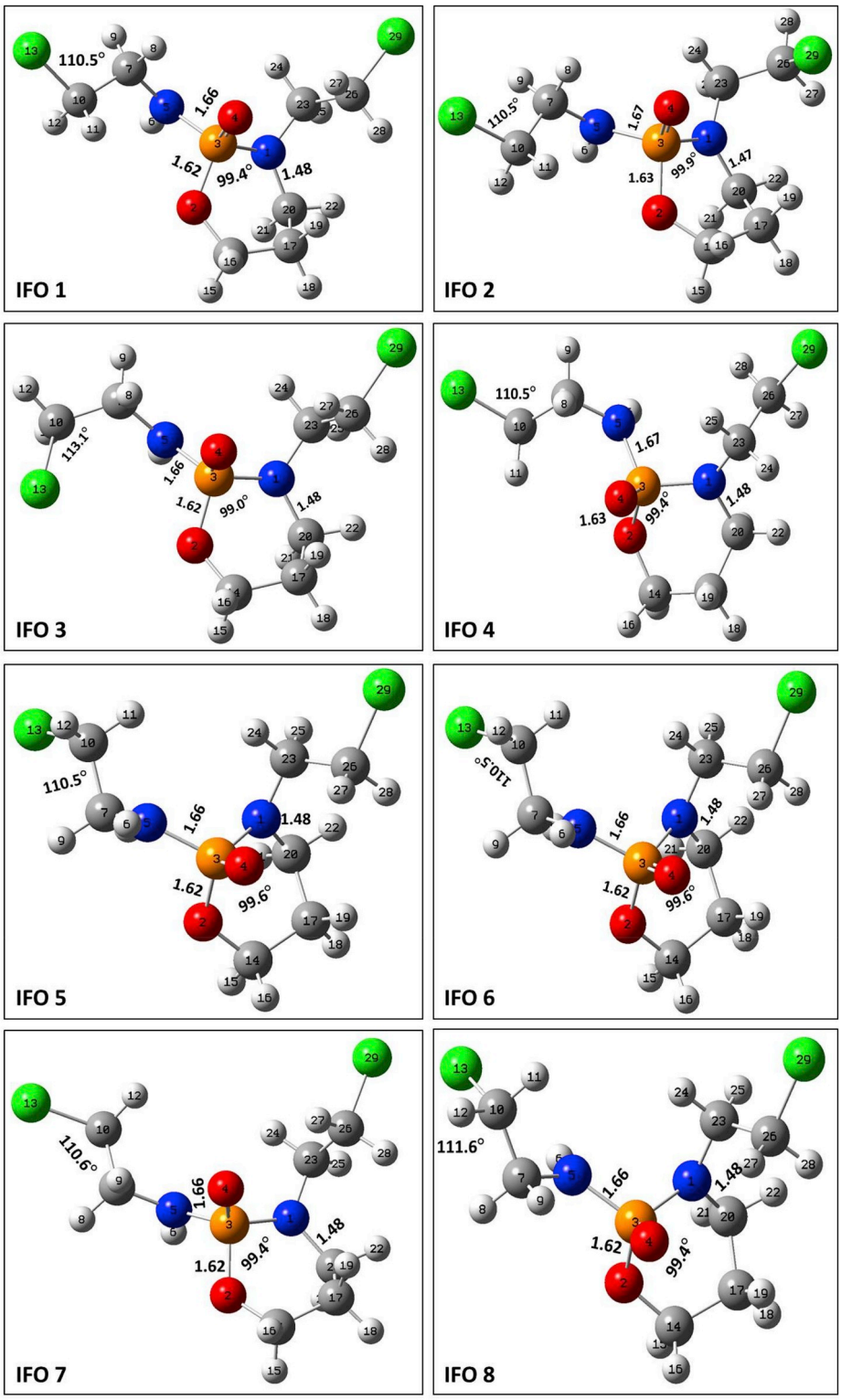

Fig. 1. B3LYP/6-311G++ fully optimized structures of IFO conformers, Atom colors: green—chlorine, white—hydrogen, blue—nitrogen, gray—carbon, orange—phosphorus and red—oxygen. The most stable conformer depicted in the border.

better improved. As a result, the biodistribution and pharmacokinetics made them soluble and biocompatible, so they may enter the cell nucleus. The drug can be attached on the external or the internal surface. Encapsulation or internalization depends on van der Waals forces and other weak interactions. However, encapsulation is sensitive to external environments [24].

SWNT-based drug delivery systems (DDS) have been widely developed. DDS could recognize specific receptors on the cancer cell surface and through specific interactions induce receptor-mediated endocytosis.

In this study, we have probed the interaction of the IFO molecule with a carbon nanotube as the drug carrier to reduce the adverse side effects and to produce a more effective drug delivery system. The atomic interactions of high polar IFO molecule and non-polar carbon nanotube

Table 1
Relative energy (Ere) in kJ/mol, the highest occupied molecular orbital (HOMO) energy, E_{HOMO}, the lowest unoccupied molecular orbital (LUMO) energy, E_{LUMO}, energy gap E_g, chemical potential, μ, chemical hardness, η, and electrophilicity, ω, for different IFO conformers in eV.

Conformer	E_{re}	E_{HOMO}(eV)	E_{LUMO}(eV)	Eg	η	μ	ω
IFO 1	4.17	−6.926	−0.704	6.222	3.111	−3.815	2.339
IFO 2	20.22	−6.805	−0.709	6.096	3.048	−3.757	2.315
IFO 3	12.39	−6.764	−0.598	6.166	3.083	−3.681	2.197
IFO 4	6.38	−6.974	−0.779	6.195	3.097	−3.877	2.426
IFO 5	4.52	−6.927	−0.636	6.291	3.146	−3.782	2.273
IFO 6	4.49	−6.928	−0.636	6.292	3.146	−3.782	2.273
IFO 7	5.80	−6.952	−0.700	6.252	3.126	−3.826	2.342
IFO 8	0	−6.862	−0.570	6.293	3.146	−3.716	2.195

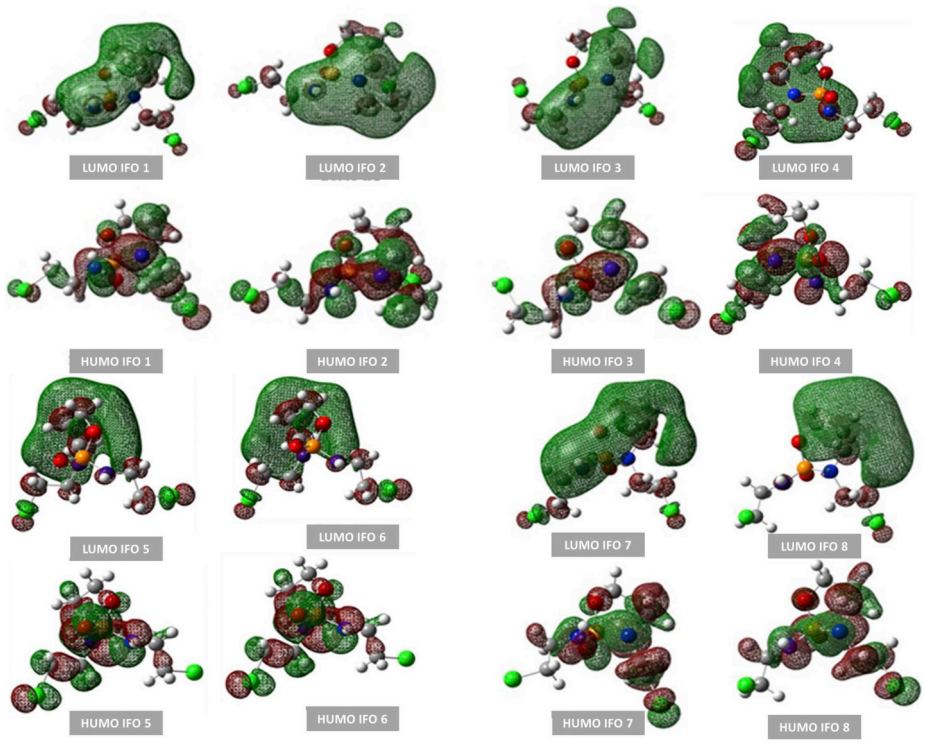

Fig. 2. The pictorial illustration of HOMO and LUMO frontier molecular orbitals for different possible conformers of Ifosfamide calculated by B3LYP method with 6–311++G(d,p).

Table 2
The structural and the topological and the hydrogen bonding energy values ($kJmol^{-1}$) in the investigated ifosfamide conformers. Topological parameters unit is a.u.

IFO Conformer	Label	bond distance(Å)	ρ_{BCP}	$\nabla^2\rho_{BCP}$	ρ_{RCP}	$\nabla^2\rho_{RCP}$	$E_{HB}(kJmol^{-1})$
1	P–O4···H27	2.681	0.0074	0.0243	0.0070	0.0286	−4.7692
3	P–O4···H27	2.677	0.0074	0.0245	0.0071	0.0288	−4.8152
5	P–O4···H27	2.628	0.0081	0.0264	0.0075	0.0312	−5.3600
6	P–O4···H27	2.628	0.0081	0.0264	0.0075	0.0312	−5.3633
7	P–O4···H27	2.679	0.0074	0.0243	0.0071	0.0286	−4.7923
8	P–O4···H27	2.693	0.0072	0.0238	0.0070	0.0279	−4.6530

have been modeled by density functional theory.

2. Computational details

The present study was performed by Gaussian 09 series of programs package [25] using the density functional theory (DFT) [26,27]. Full geometry optimization was computed at the same level to find the most stable conformer of IFO which then selected to be used in the encapsulation process. The structures have been indicated to be minima since no imaginary frequency have been reported. The quantum theory of atoms in molecule (QTAIM) [28] and the IR analysis of all the conformers have been also performed. Espinosa [29] method has been utilized to investigate the intramolecular hydrogen bonding (HB). After that, a segment of (10,10) armchair SWCNT, containing 200 carbon atoms and 40 hydrogen atoms, with 13.465 Å diameter was chosen as a model for encapsulation of IFO. The adsorption energies, for the IFO encapsulated in pristine SWCNT (IFO@SWCNT) were calculated as:

$$E_{ads} = E_{(IFO@SWCNT)} - [E_{(SWCNT)} + E_{(IFO)}] \quad (1)$$

E_{ads} is the adsorption energy, E(IFO@SWCNT) is the total energy obtained from the optimized structure of IFO encapsulated within SWCNT, $E_{(SWCNT)}$, and $E_{(IFO)}$ are the total energies of pristine SWCNT

Table 3
Calculated stretching vibrations of intramolecular hydrogen bonds formed in IFO conformers (cm^{-1}).

Conformer	Stretching Frequency			
	C26–H27···O4	N5–H6	P3=O4	C26–Cl29
IFO1	3160.71	3594.33	1227.34	740.92
IFO2	3133.97	3584.2	1259.79	655.2
IFO3	3161.23	3598.76	1225.85	738.28
IFO4	3149.55	3588.21	1225.56	744.78
IFO5	3161.92	3600.36	1223.73	741.75
IFO6	3161.93	3600.33	1223.72	741.76
IFO7	3160.86	3594.44	1227.85	742.28
IFO8	3159.83	3586.22	1222.58	738.94

and the IFO respectively. The frontier molecular orbitals, the highest occupied molecular orbital (HOMO) and the lower unoccupied molecular orbital (LUMO) analysis were studied to estimate the binding scheme and chemical stability of the mentioned system. Further, the electronic structure can be characterized by the frontier molecular orbital energies: E_{HOMO} and E_{LUMO}. The LUMO as electron acceptor shows the ability to obtain electron and HOMO shows the ability to donate an electron. The energy gap between HOMO and LUMO (ΔE_g) as the stability index has been calculated. The DFT-based stability and reactivity descriptors [30] have been evaluated according to the following equation.

$$\mu = \left(\frac{\partial E}{\partial N}\right)_{V(r),T} \tag{2}$$

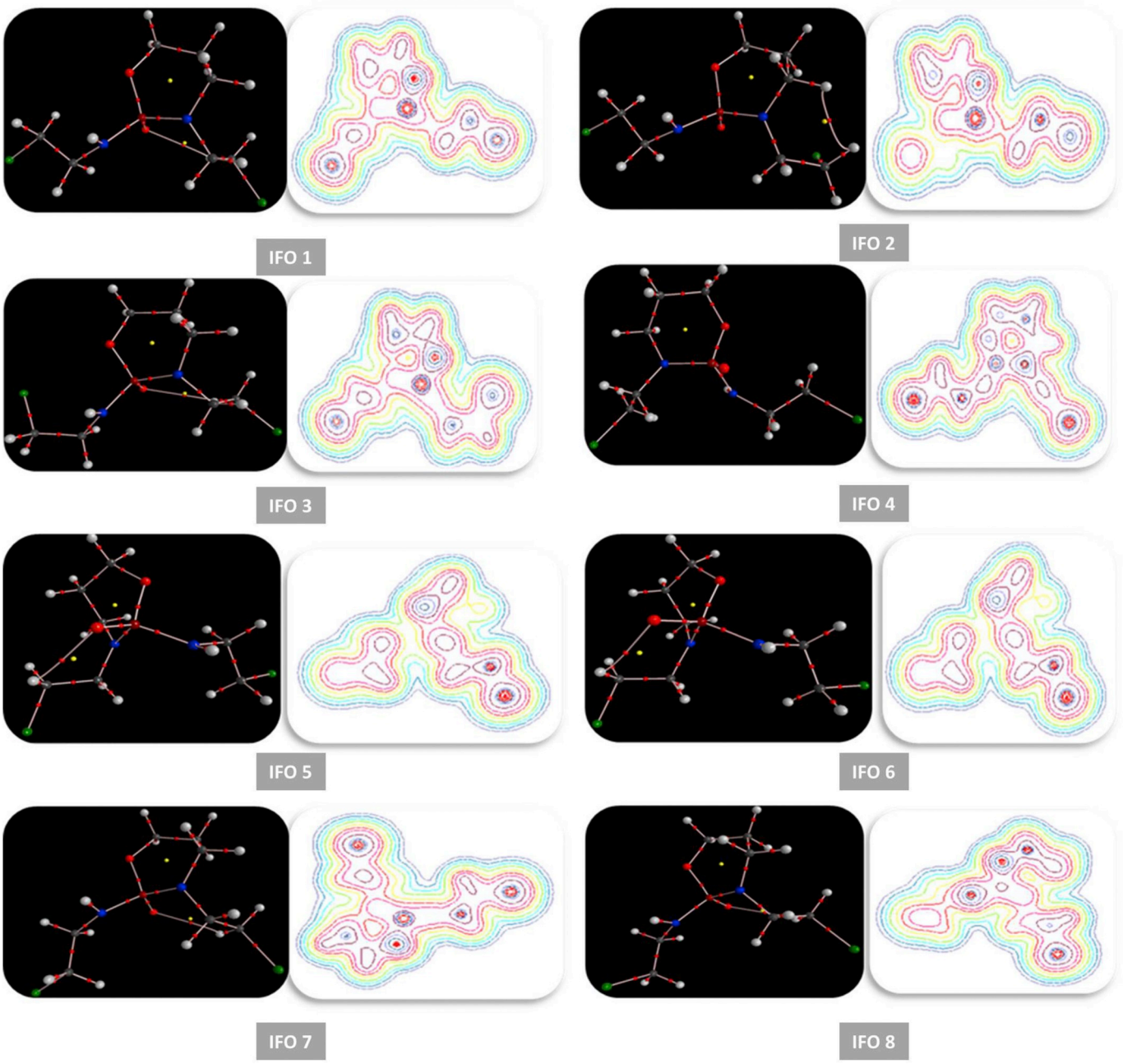

Fig. 3. The molecular graph and contour map of IFO conformers.

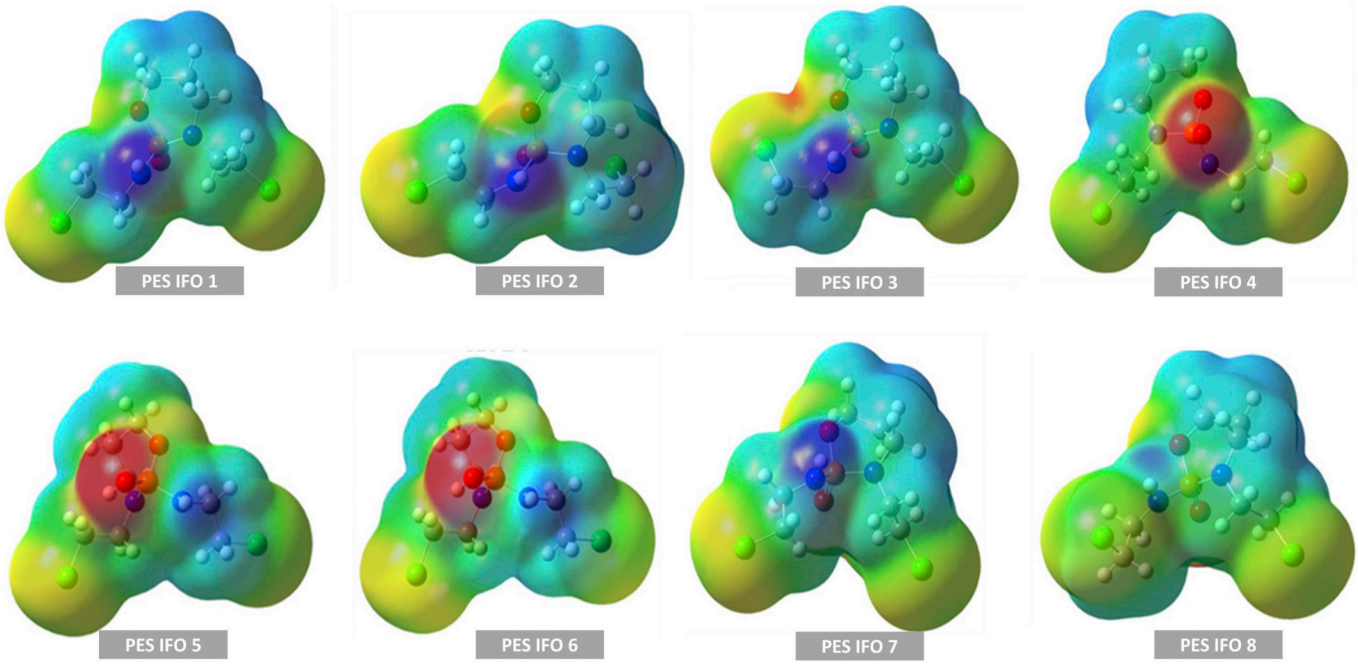

Fig. 4. The electron density isosurfaces for different possible conformers of Ifosfamide calculated by B3LYP method with 6–311++G(d,p) basis set.

Table 4
DFT based descriptors of IFO in different solvents. Units are in eV.

DFT descriptors	Water	DMSO	Ethanol	Acetone	CCl4
E_{HOMO} (ev)	−6.786	−6.787	−6.790	−6.791	−6.828
E_{LUMO} (ev)	−0.312	−0.313	−0.316	−0.318	−0.423
$\Delta E_{HOMO\text{-}LUMO}$ (ev)	6.474	6.474	6.473	6.473	6.405
Chemical potential (μ) (ev)	−3.549	−3.550	−3.553	−3.554	−3.625
Chemical hardness(η) (ev)	3.237	3.237	3.237	3.236	3.203
Electrophilicity index	1.945	1.947	1.950	1.952	2.052

$$\eta = \left(\frac{\partial^2 E}{\partial N^2}\right)_{V(r),T} \tag{3}$$

where μ is the chemical potential and η is chemical hardness. Parr [31] introduced the global electrophilicity index using the chemical potential and chemical hardness:

$$\omega = \mu^2/\eta^2 \tag{4}$$

3. Result

3.1. Conformational and IR analysis of Ifosfamide

All possible conformations of IFO heterocyclic compound have been investigated using DFT/B3LYP/6–31++G(d, p) level of theory to determine the most stable conformer to clarify the molecular structure in the encapsulation process. All possible conformers of IF are depicted in Fig. 1.

Regarding the conformer's standard theoretical classification, IFO molecule has eight conformers and their energies are listed in Table 1.

The frontier molecular orbital, HOMO and LUMO, representations for the conformers have been shown in Fig. 2.

ΔE_g defines the molecular electric transport properties. The DFT based chemical stability and reactivity descriptors such as energy gap (E_g), chemical potential, chemical hardness (η) and electrophilicity index (ω) were calculated regarding the molecular orbital energy values (see Table 1). As shown, the relatively high value of E_g shows that the studied conformers display high chemical stability. IFO8 conformer is

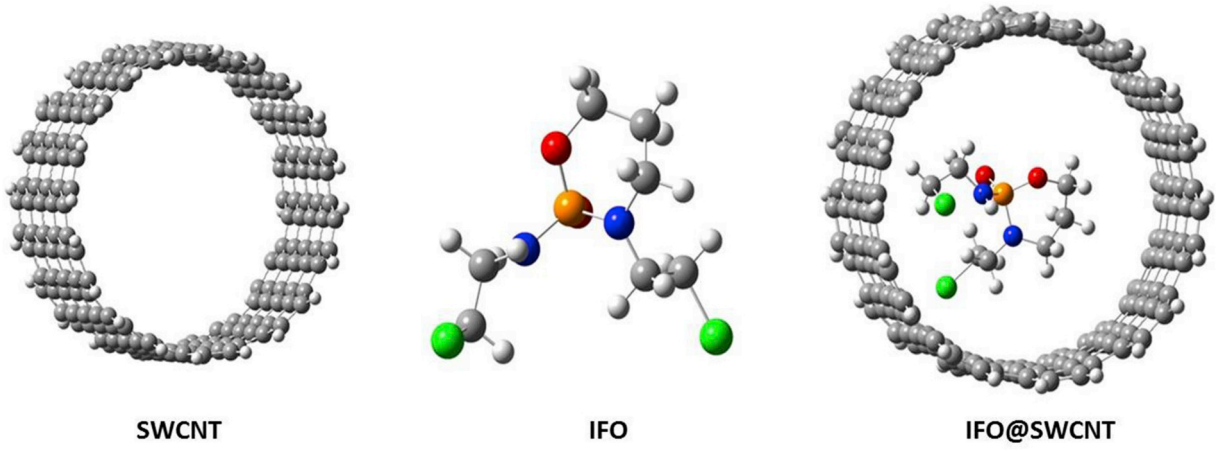

Fig. 5. Optimized structure of the most stable SWCNT, IFO and IFO@SWCNT

Table 5
Geometric parameters of the most stable IFO conformer before and after the encapsulation process. Units are in Å.

IFO bond	Before encapsulation	After encapsulation
N1–C20	1.47769	1.47638
N1–P3	1.68049	1.68834
N1–C23	1.46406	1.46472
P3–O2	1.62322	1.62983
P3–N5	1.65889	1.66905
O2–C14	1.44968	1.45500
C14–C17	1.53286	1.53566
C17–C20	1.53335	1.53972
C7–C10	1.51742	1.51496
C23–C26	1.52995	1.52856
N5–C7	1.46091	1.46331
C10–Cl13	1.82585	1.90810
C26–Cl29	1.81926	1.91128
P3–O4	1.48780	1.54411

the hardest conformer with the highest energy gap value whereas IFO2 conformer is the softest and the most polarizable one which are confirmed with the DFT based chemical indexes.

The characteristics of corresponding bond critical points (BCP) are also studied for investigated conformers. To get deeper insight into the characteristics of intra-molecular hydrogen bonds (H-Bonds), Espinosa method has been utilized to analyze the HB. The pseudo-ring containing P–O···H intra-molecular HB is formed and therefore the RCP also exists. The parameters of the critical points of the studied molecules are presented in Table 2. It is worth inferring that the greater electron density at BCP of intera-molecular HB corresponds to the stronger interaction. For example, P–O4···H27 bond in IFO 6 conformer has the greater electron density and HB energy too. The positive Laplacian that is the topological testimony of the non-covalency of closed shell interactions, could be found in the listed results. The electron density at the corresponding bond reflects the strength of any pair interactions. The weakened intra-molecular HB have been formed in the most stable conformer.

Quantum theory of atom in molecule, which characterizes the bonds by a topological analysis of electronic charge density and their Laplacian

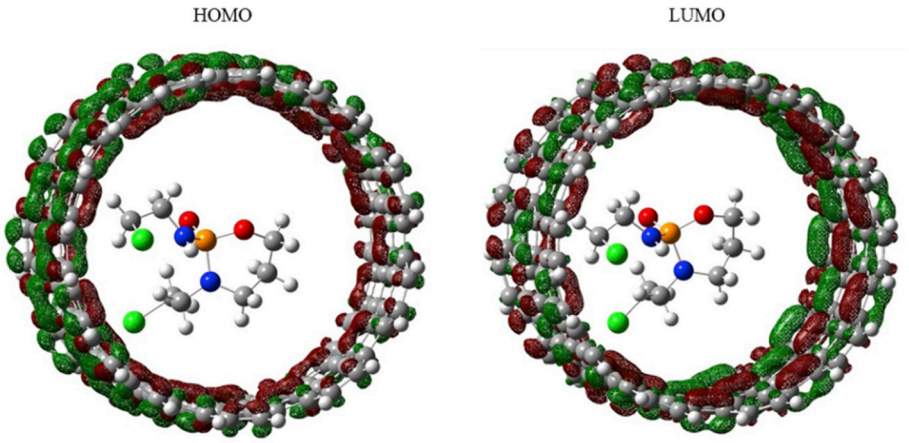

Fig. 6. The calculated HOMO and LUMO orbitals localized on the SWCNT.

Table 6
Total energy, ET, and DFT descriptors of isolated and encapsulated IFO into the considered SWCNT. Units are in eV.

	E_T	E_{HOMO}	E_{LUMO}	E_g	η	μ	ω
IFO	−1797.204	−6.862	−0.57	6.292	3.146	−3.716	2.195
SWCNT	−7644.753	−4.460	−2.502	1.958	0.979	−3.481	6.190
IFO@SWCNT	−9442.100	−4.696	−2.461	2.235	1.118	−3.578	5.728

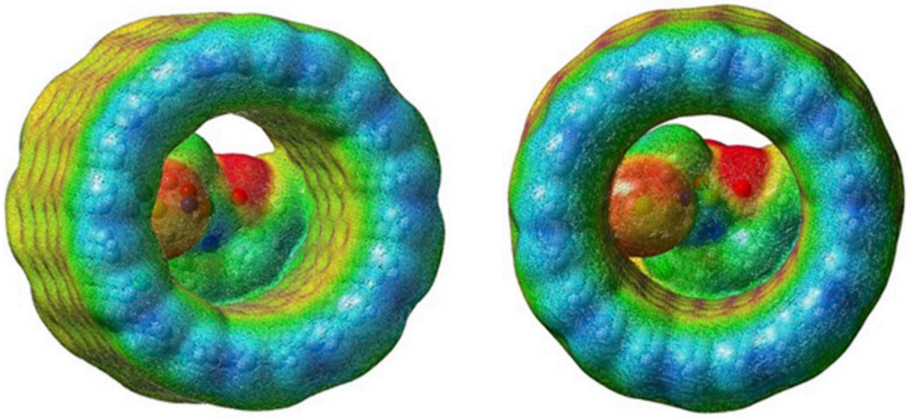

Fig. 7. The electron density isosurfaces for the IFO@SWCNT (10, 10) calculated by B3LYP method with 6–311++G(d,p) basis set.

at the bond critical point (BCP) [32–34], were done. Fig. 3 shows the contour map and molecular graph of IFO conformers. Regions of concentration of electron in the contour map diagram show the isodensity around the electronegative atoms that incorporate in the strong interactions. The electron density at BCP is often used as a scale of the HB strength and it correlates well with the HB energy. The results of topological analysis presented the positive values of charge densities and their Laplacians which referred to non-covalent HB interactions. The ρ_{RCP} parameter correlates well with the other properties of intramolecular H-bonds which are recognized as useful measures of the H-bond strength.

Molecular electrostatic potential map was constructed by Gauss View 5.0. The electron density isosurfaces for all investigated molecules are presented in Fig. 4. Different colors visualize the different electrostatic potentials at the surface. The area of repulsion potential appears in blue and that of attractive potential appear in red.

Results of IR analysis of the studied conformers (see Table 3) showed that strong HB are characterized by stretching frequencies above 3100 cm^{-1}. The correlation of increasing H···O stretching frequency with attenuates the O–H bond strength could be found.

The solvent effects on the DFT based descriptors of the most stable conformer of IFO have been investigated in ethanol, DMSO, water, carbon tetrachloride and acetone (Table 4). It could be found that by increasing the dielectric constant of the solvents, no significant changes occur in the stability and reactivity of the conformer.

3.2. Encapsulation of Ifosfamide into single-walled carbon nanotubes

In order to analyze how the encapsulation influences the electronic properties of the molecules, first the IFO molecule was placed in the center of the carbon nanotube's interior and then optimization of the whole structure was performed. The interactions between single-walled carbon nanotubes and IFO have been evaluated by DFT calculations. The chemical bonds obtained between the molecule and its carrier increase the geometric stability of the anticancer agent.

To gain this aim, the most stable conformer of IFO, IFO 8, has been encapsulated in optimized geometry of SWCNT and the resulted complex (IFO@SWCNT) has been fully optimized at B3LYP/6–311++G(d,p) level of theory. Fig. 5 shows the above mentioned optimized structures.

The adsorption energy value of −3.87 eV, calculated using Eq. (1), shows the exothermic behavior of the adsorption and indicates that the interaction is spontaneous.

The interaction between IFO and SWCNT in terms of their bond distances could be verified from the comparing of the bonds length in the isolated IFO with those of the encapsulated molecule into the SWCNT. Small changes were seen at the adsorption process for the IFO molecule bonds (Table 5). In addition, the comparison of the calculated CNTs diameters before and after the incorporation of the IFO, reveals that nanotubes diameters were enlarged after the encapsulation from 13.46 Å to 13.82 Å.

DFT calculations for the IFO@SWCNT complexes show that the HOMO and LUMO orbitals are localized on SWCNT (Fig. 6). Red and green colors represent the positive and negative phases, respectively. After encapsulation, in SWCNT, all of C–H bonds are completely antibonding orbitals and C–C bonds are boning orbitals. This confirms no significant charge transfer from the IFO molecule toward the SWCNT through the encapsulation process.

From the energy gap values, it is inferred that IFO has decreased the reactivity of the SWCNT because the chemical hardness values increase compared to that of the pristine form. Besides, the encapsulated SWCNT have lower energy gap values compared to their pristine counterparts. Results listed in Table 6 show that the encapsulation of IFO seems to have decreased the chemical potential and electrophilicity index of the pristine SWCNT. Higher chemical hardness indicates the structural stability and lower electrophilicity index could be a good descriptor of lower toxicity.

The changes of nucleophile and electrophile sites after encapsulation are presented in Fig. 7. Total electron density maps of the electronic densities (Fig. 7) demonstrate that IFO strongly bonded to the interior side of SWCNT that previously predicted in terms of binding energy.

4. Discussion

Carbon nanotubes as nanocarriers for encapsulation of drug play an important role in novel medical treatments. In this study, we have theoretically investigated the encapsulation efficiency of SWCNT through the interaction of Ifosfamide molecule with the interior sidewall of SWCNT using DFT calculations.

Several models have been considered to characterize the encapsulated systems. Tang and Yang [35] described the encapsulation of C60 molecules in SWCNT in solvent conditions by means of molecular dynamic simulation and they have demonstrated the ability of inserting these molecules in the nanotube in good agreement with experimental results. Encapsulation of organic molecules in SWCNTs is one of the possible reasons for the stability, since the outer wall of SWCNTs will protect the molecule from oxygen [36].

An important difference between molecular adsorption and encapsulation in SWCNTs is van der Waals interactions which made the encapsulation a reversible process and also the atomic structure does not alter. Lewis J.P. et al. [37] and Jelinek P. et al. [38] groups have described the DFT computational scheme of the interaction in details. Russo R. et al. [39] have studied the structural properties and thermal stability of metallo-fullerene encapsulated in CNTs which opens the way for study of such super molecular structures. Mandal B. et al. [40] characterized the encapsulation of graphene nanoribbons in zig-zag SWCNTs of different size theoretically and they have shown that the nanoribbon encapsulation in a nanotube could be possible.

Joko Y. et al. [41] have investigated the encapsulation of coronene molecules into a SWCNT using molecular dynamic method and they have shown that through the process the concave-concave dimers formed which is because of the van der Waals interactions between convex surface of molecule and the inner wall of SWCNT.

The encapsulation of anticancer Cisplatin in carbon nanotube have been studied by Mejri A. et al. [42] and results showed high storage capacity of CNT, and also that it is not necessary to close their both ends. Also the release of drugs can be favored near the membrane cell due to advantageous electrostatic interactions with the hydrophilic part of the cell.

5. Conclusion

We have calculated the binding energy and equilibrium bonding distances for the full optimized complex of IFO@SWCNT after determination of the most stable conformer of Ifosfamide within eight possible conformers. Results have shown that the suitable SWCNT for the encapsulation of IFO has a diameter of about 13.456 Å. The adsorption energy value implies that the IFO adsorbs onto interior walls of the SWCNT through a chemisorption process. Overall, SWCNT could be a suitable candidate for the encapsulating of IFO drug with lower toxicity.

Acknowledgements

The authors wish to thank Graduate University of Advanced Technology, Kerman, Iran, for their support.

References

[1] B. Giraud, G. Hebert, A. Deroussent, G.J. Veal, G. Vassal, A. Paci, Oxazaphosphorines: new therapeutic strategies for an old class of drugs, Expert Opin. Drug Metabol. Toxicol. 6 (2010) 919–938.
[2] Y. Fukumori, H. Ichikawa, Nanoparticles for cancer therapy and diagnosis, Adv. Powder Technol. 17 (2006) 1–28.

[3] A.H. Faraji, P. Wipf, Nanoparticles in cellular drug delivery, Bioorg. Med. Chem. 17 (2009) 2950–2962.
[4] M. Yoosefian, N. Etminan, Density functional theory (DFT) study of a new novel bionanosensor hybrid; tryptophan/Pd doped single walled carbon nanotube, Phys. E Low-dimens. Syst. Nanostruct. 81 (2016) 116–121.
[5] N. Etminan, M. Yoosefian, H. Raissi, M. Hakimi, Solvent effects on the stability and the electronic properties of histidine/Pd-doped single-walled carbon nanotube biosensor, J. Mol. Liq. 214 (2016) 313–318.
[6] H. Ai, S.A. Jones, M.M. de Villiers, Y.M. Lvov, Nano-encapsulation of furosemide microcrystals for controlled drug release, J. Control. Release 86 (2003) 59–68.
[7] R. Pandey, Z. Ahmad, S. Sharma, G. Khuller, Nano-encapsulation of azole antifungals: potential applications to improve oral drug delivery, Int. J. Pharm. 301 (2005) 268–276.
[8] I.G. Loscertales, A. Barrero, I. Guerrero, R. Cortijo, M. Marquez, A. Ganan-Calvo, Micro/nano encapsulation via electrified coaxial liquid jets, Science 295 (2002) 1695–1698.
[9] M. Yoosefian, Z. Ansarinik, N. Etminan, Density functional theory computational study on solvent effect, molecular conformations, energies and intramolecular hydrogen bond strength in different possible nano-conformers of acetaminophen, J. Mol. Liq. 213 (2016) 115–121.
[10] E. Mirhaji, M. Yoosefian, Structural analysis, solvent effects and intramolecular interactions in rilpivirine: a new non-nucleoside reverse transcriptase inhibitor for HIV treatment, J. Mol. Liq. 246 (2017) 124–130.
[11] F. Mollaamin, M. Monajjemi, DFT outlook of solvent effect on function of nano bioorganic drugs, Phys. Chem. Liq. 50 (2012) 596–604.
[12] T.A. Hilder, J.M. Hill, Modelling the encapsulation of the anticancer drug cisplatin into carbon nanotubes, Nanotechnology 18 (2007) 275704.
[13] S. Iijima, Helical microtubules of graphitic carbon, Nature 354 (1991) 56–58.
[14] W. Yang, P. Thordarson, J.J. Gooding, S.P. Ringer, F. Braet, Carbon nanotubes for biological and biomedical applications, Nanotechnology 18 (2007) 412001.
[15] Y. Zhang, Y. Bai, B. Yan, Functionalized carbon nanotubes for potential medicinal applications, Drug Discov. Today 15 (2010) 428–435.
[16] B.I. Yakobson, P. Avouris, Mechanical Properties of Carbon Nanotubes, Carbon Nanotubes, Springer, 2001, pp. 287–327.
[17] C. Journet, W. Maser, P. Bernier, A. Loiseau, M.L. De La Chapelle, d.l.S. Lefrant, P. Deniard, R. Lee, J. Fischer, Large-scale production of single-walled carbon nanotubes by the electric-arc technique, Nature 388 (1997) 756–758.
[18] T. Ebbesen, H. Lezec, H. Hiura, J. Bennett, H. Ghaemi, T. Thio, Electrical conductivity of individual carbon nanotubes, Nature 382 (1996) 54–56.
[19] M. Yoosefian, N. Etminan, The role of solvent polarity in the electronic properties, stability and reactivity trend of a tryptophane/Pd doped SWCNT novel nanobiosensor from polar protic to non-polar solvents, RSC Adv. 6 (2016) 64818–64825.
[20] D. Pantarotto, J.-P. Briand, M. Prato, A. Bianco, Translocation of bioactive peptides across cell membranes by carbon nanotubes, Chem. Commun. (2004) 16–17.
[21] A.D. Franklin, S.O. Koswatta, D.B. Farmer, J.T. Smith, L. Gignac, C.M. Breslin, S.-J. Han, G.S. Tulevski, H. Miyazoe, W. Haensch, Carbon nanotube complementary wrap-gate transistors, Nano Lett. 13 (2013) 2490–2495.
[22] M. Yoosefian, M. Jahani, A molecular study on drug delivery system based on carbon nanotube for the novel norepinephrine prodrug, Droxidopa, J. Mol. Liq. 284 (2019) 258–264.
[23] M. Yoosefian, E. Rahmanifar, N. Etminan, Nanocarrier for levodopa Parkinson therapeutic drug; comprehensive benserazide analysis, Artif. Cells Nanomed. Biotechnol. 46 (2018) 434–446.
[24] A. Bianco, K. Kostarelos, C.D. Partidos, M. Prato, Biomedical applications of functionalised carbon nanotubes, Chem. Commun. (2005) 571–577.
[25] M. Frisch, G. Trucks, H.B. Schlegel, G. Scuseria, M. Robb, J. Cheeseman, G. Scalmani, V. Barone, B. Mennucci, G. Petersson, Gaussian 09, Revision A. 02, Gaussian, Inc., Wallingford, CT, 2009, p. 200.
[26] A.D. Becke, Density-functional thermochemistry. III. The role of exact exchange, J. Chem. Phys. 98 (1993) 5648–5652.
[27] C. Lee, W. Yang, R.G. Parr, Development of the Colle-Salvetti correlation-energy formula into a functional of the electron density, Phys. Rev. B 37 (1988) 785–789.
[28] R.F. Bader, Atoms in Molecules: A Quantum Theory, Oxford University Press, Oxford, 1990.
[29] E. Espinosa, E. Molins, C. Lecomte, Hydrogen bond strengths revealed by topological analyses of experimentally observed electron densities, Chem. Phys. Lett. 285 (1998) 170–173.
[30] T. Koopmans, Über die Zuordnung von Wellenfunktionen und Eigenwerten zu den einzelnen Elektronen eines Atoms, Physica 1 (1934) 104–113.
[31] R.G. Parr, L.v. Szentpaly, S. Liu, Electrophilicity index, J. Am. Chem. Soc. 121 (1999) 1922–1924.
[32] O.h.O. Brovarets, D.M. Hovorun, Atomistic mechanisms of the double proton transfer in the H-bonded nucleobase pairs: QM/QTAIM computational lessons, J. Biomol. Struct. Dyn. (2018) 1–28.
[33] O.B. Ol'ha, I.S. Voiteshenko, H. Pérez-Sánchez, D.M. Hovorun, A QM/QTAIM research under the magnifying glass of the DPT tautomerisation of the wobble mispairs involving 2-aminopurine, New J. Chem. 41 (2017) 7232–7243.
[34] O.B. Ol'ha, R.O. Zhurakivsky, D.M. Hovorun, The physico-chemical "anatomy" of the tautomerization through the DPT of the biologically important pairs of hypoxanthine with DNA bases: QM and QTAIM perspectives, J. Mol. Model. 19 (2013) 4119–4137.
[35] L. Tang, X. Yang, Molecular dynamics simulation of C60 encapsulation into single-walled carbon nanotube in solvent conditions, J. Phys. Chem. C 116 (2012) 11783–11791.
[36] Y.J. Dappe, Encapsulation of organic molecules in carbon nanotubes: role of the van der Waals interactions, J. Phys. D Appl. Phys. 47 (2014), 083001.
[37] J.P. Lewis, K.R. Glaesemann, G.A. Voth, J. Fritsch, A.A. Demkov, J. Ortega, O. F. Sankey, Further developments in the local-orbital density-functional-theory tight-binding method, Phys. Rev. B 64 (2001) 195103.
[38] P. Jelínek, H. Wang, J.P. Lewis, O.F. Sankey, J. Ortega, Multicenter approach to the exchange-correlation interactions in ab initio tight-binding methods, Phys. Rev. B 71 (2005) 235101.
[39] R. Russo, B.W. Smith, B. Satishkumar, D.E. Luzzi, H.C. Dorn, Encapsulated molecules in carbon nanotubes: structure and properties, MRS Online Proc. Libr. Arch. (2001) 675.
[40] B. Mandal, S. Sarkar, P. Sarkar, Energetics and electronic structure of encapsulated graphene nanoribbons in carbon nanotube, J. Phys. Chem. A 117 (2013) 8568–8575.
[41] Y. Joko, R. Sasaki, K. Shintani, Dynamic encapsulation of corannulene molecules into a single-walled carbon nanotube, Phys. Chem. Chem. Phys. 19 (2017) 27704–27715.
[42] A. Mejri, D. Vardanega, B. Tangour, T. Gharbi, F. Picaud, Encapsulation into carbon nanotubes and release of anticancer cisplatin drug molecule, J. Phys. Chem. B 119 (2015) 604–611.